Nexo Revista Científica
Vol. 36, No. 03, pp. 272-294/Junio 2023

ISSN-E 1995-9516
Universidad Nacional de Ingeniería

http://revistas.uni.edu.ni/index.php/Nexo
https://doi.org/10.5377/nexo.v36i03.16448

Thermo-hydraulic rating of a gasketed-plate heat exchanger for methanol heating

Evaluación térmico-hidráulica de un intercambiador de calor de placas para el calentamiento de metanol

Amaury Pérez Sánchez [1,*], Helen María Alfonso Fernández [1], Greisy Ivety Valero Almanza [2], Elizabeth Ranero González [1], Eddy Javier Pérez Sánchez[3]

[1] Universidad de Camagüey "Ignacio Agramonte Loynaz", Facultad de Ciencias Aplicadas, Departamento de Ingeniería Química, Camagüey, Cuba.
[2] Centro de Ingeniería Ambiental de Camagüey, Departamento de Gestión Ambiental, Camagüey, Cuba.
[3] Empresa Servicios Automotores S.A., Dirección Comercial, Ciego de Ávila, Cuba.
[*]amaury.perez84@gmail.com

(recibido/received: 15-enero-2023; aceptado/accepted: 12-abril-2023)

ABSTRACT

The use of plate heat exchangers is desirable since they have a simple compact construction, are reliable, and very efficient at small temperature difference between fluids. In the present work the thermo-hydraulic rating of a proposed gasketed-plate heat exchanger was carried out, in order to heat a methanol stream. A safety factor of 1.62, a percent over surface of 3.91% and a cleanliness factor of 0.962 was obtained. The calculated values of the pressure drops for both the hot water and methanol streams were 47,199.05 Pa and 78,414.61 Pa, respectively, while the pumping power required for those both streams were 4.81 kW and 11.38 kW, respectively. The proposed gasketed-plate heat exchanger can be used for the requested heat transfer service since the percent over surface is lower than 25% and the calculated pressure drop of both streams are below the maximum permissible pressure drop established by the process.

Keywords: Gasketed-plate heat exchanger; Methanol; Percent over surface; Pressure drop; Rating.

RESUMEN

El empleo de intercambiadores de calor de placas es deseable ya que poseen una construcción compacta simple, son confiables y muy eficientes para una pequeña diferencia de temperatura entre los fluidos. En el presente trabajo se llevó a cabo la evaluación térmico-hidráulica de un intercambiador de calor de placas propuesto, con el fin de calentar una corriente de metanol. Se obtuvo un factor de seguridad de 1,62, un porciento de sobre superficie de 3,91% y un factor de limpieza de 0,962. Los valores calculados de las caídas de presión para tanto las corrientes de agua caliente y metanol fueron de 47 199,05 Pa y 78 414,61 Pa, respectivamente, mientras que la potencia de bombeo requerida para ambas corrientes fueron 4,81 kW y 11,38 kW, respectivamente. El intercambiador de calor de placas propuesto puede ser empleado para el servicio de transferencia de calor requerido debido a que el porciento de sobre superficie

es menor que 25% y la caída de presión calculada de ambas corrientes están por debajo de la caída de presión máxima permisible establecida por el proceso.

Palabras claves: Intercambiador de calor de placas; Metanol; Porciento de sobre superficie; Caída de Presión; Evaluación.

NOMENCLATURE

A_1	Single-plate heat transfer area	m^2
A_{1p}	Projected plate area	m^2
A_{ch}	One channel flow area	m^2
A_e	Total effective area	m^2
b	Mean channel flow gap	m
CF	Cleanliness factor	-
C_h	Heat transfer constant	-
Cp	Specific heat	J/kg.K
C_s	Safety factor	-
D_h	Channel hydraulic/equivalent diameter	m
D_p	All port diameters	m
f	Friction coefficient	-
G	Mass velocity	$kg/m^2.s$
G_{ph}	Port mass velocity	$kg/m^2.s$
h	Film heat transfer coefficient	$W/m^2.K$
k	Thermal conductivity	W/m.K
k_p	Thermal conductivity of the plate material	W/m.K
K_p	Pressure drop coefficient	-
L_c	Compressed plate pack length	m
L_{eff}	Effective flow length between the vertical ports	m
L_h	Horizontal port distance	m
L_v	Vertical port distance	m
L_w	Effective channel width	m
m	Mass flowrate	kg/s
m	Pressure drop coefficient	-
m_c	Mass flowrate per channel	kg/s
n	Heat transfer constant	-
N_{cp}	Number of channels per pass	-
N_e	Effective number of plates	-
N_p	Number of passes	-
N_t	Total number of plates	-
OS	Percent over surface design	%

p	Plate pitch	m
P	Pumping power	W
Pr	Prandtl number	-
ΔP	Total pressure drop	Pa
ΔP_f	Frictional pressure drop	Pa
ΔP_m	Maximum permissible pressure drop	Pa
ΔP_p	Pressure drop in the port ducts	Pa
Q	Required heat load	W
Q_C	Actual heat duty for clean surface	W
Q_F	Actual heat duty for fouled surface	W
R	Fouling factor	m^2.K/W
Re	Reynolds number	-
t	Temperature of the cold fluid	ºC
t_p	Plate thickness	m
$\bar{t}$	Mean temperature of the cold fluid	ºC
T	Temperature of the hot fluid	ºC
$\bar{T}$	Mean temperature of the hot fluid	ºC
ΔT_m	Mean temperature difference	ºC
U_C	Clean overall heat transfer coefficient	W/m^2.K
U_F	Fouled overall heat transfer coefficient	W/m^2.K
	Greek symbols	
β	Chevron angle	º
ϕ	Enlargement factor	-
ρ	Density	kg/m^3
μ	Viscosity	Pa.s
η_p	Isentropic efficiency of the adiabatic pump	-
	Subscripts	
1	Inlet	
2	Outlet	
c	Cold fluid	
h	Hot fluid	
w	At the wall temperature	

1. INTRODUCTION

Heat exchangers are devices used to transfer energy between two fluids at different temperatures. They improve energy efficiency, because the energy already within the system can be transferred to another part of the process, instead of just being pumped out and wasted (Mota *et al*., 2015).

Heat exchangers could be classified in many different ways such as according to transfer processes, number of fluids, surface compactness, flow arrangements, heat transfer mechanisms, type of fluids (gas-gas, gas-liquid, liquid-liquid, gas-two-phase, liquid-two phase, etc.) and industry (Thonon & Breuil, 2000).

A plate heat exchanger (PHE) is a compact type of heat exchanger that uses a series of thin plates to transfer heat between two fluids.

PHEs were first introduced in 1923 for milk pasteurization applications, but are now used in many applications in the chemical, petroleum, HVAC, refrigeration, dairy, pharmaceutical, beverage, liquid food and health care sectors. This is due to the unique advantages of PHEs, such as flexible thermal design (plates can be simply added or removed to meet different heat duty or processing requirements), ease of cleaning to maintain strict hygiene conditions, good temperature control (necessary in cryogenic applications), and better heat transfer performance (Mota *et al*., 2015). Another advantage of the PHEs is the greatly reduced space requirements. The surface area required for a PHE is 30–50% that of a shell-and-tube heat exchanger for a given heat duty, thus in turn reducing the cost (Li *et al*., 2011).

It is believed that heat transfer coefficients are high in PHEs due to small hydraulic diameter and strong interaction between the flow inside the channel and over the corrugation crest, accompanied by the secondary flows (Heggs *et al*., 1997; Dovic *et al*., 2009), as (1) they increase turbulence and advection of fluid from the center of the channel to the near wall region; (2) they are responsible for the breakup and separation of the boundary layer and its new formation and reattachment (Elshafei *et al*., 2010); (3) they decrease the probability of appearance of stagnation areas and fouling to 10–25% of that of a shell-and-tube heat exchanger (Shah & Sekulic, 2003).

The area density of PHE ranges from 120 to 660 m^2/m^3 (Shah & Sekulic, 2003). The hydraulic diameter lies between 2 and 10 mm for most plates, and the plate size ranges from 0.02 m^2 to over 3 m^2 with conventional pressing technology, but can reach up to 15 m^2 for explosion formed plates. Typically, the number of plates is between 10 and 100, which gives 5–50 channels per fluid (Thonon & Breuil, 2000).

There are four main types of PHE: gasketed, brazed, welded, and semi-welded (Mota *et al*., 2015). The gasketed plate heat exchanger (GPHE) consists of a pack of gasketed corrugated metal plates, pressed together in a frame (Figure 1), and were introduced to simplify the task of cleaning in food industry (Hajabdollahi et al., 2016).

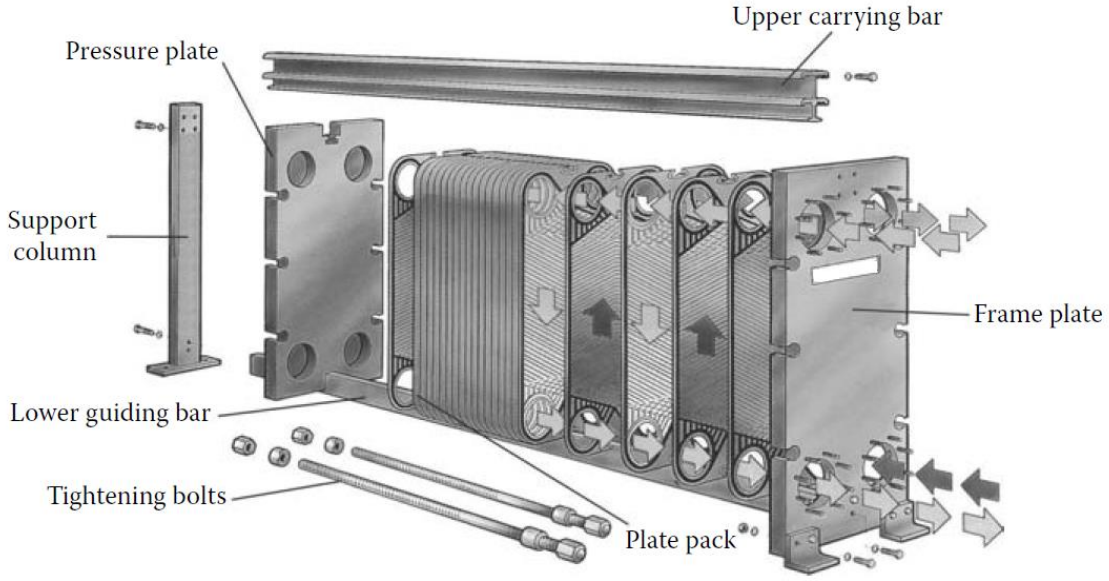

Figure 1. Gasketed-plate heat exchanger

Source: Adapted from (Kakaç et al., 2012)

The fluids flow through a series of parallel flow channels and exchange heat through the thin corrugated metal plates. The corrugations on adjacent plates contact or cross each other forming highly interrupted and tortuous channels. The gasket design and the closed ports of the plates determine the fluid flow arrangement, which can be parallel, in series or one of several possible combinations of the two. The flow distribution, number of plates, type of gaskets and feed locations characterize the exchanger configuration (Pinto & Gut, 2002). In addition, multi-pass can be accommodated by blanking plates within the stack. Various specifications can be matched by adding or removing some plates or with different plate patterns (Li *et al*., 2011).

Corrugated plate patterns cause high turbulence so that the overall heat transfer coefficient is 3-5 times greater than a shell-and- tube heat exchanger. Heat transfer coefficient can be equal to the values for tubes in which the Reynolds numbers are 5 times higher, and 3-4 times higher than that for smooth channels can be achieved (Würfel & Ostrowski, 2004).

In recent years, there is an increase in the usage of GPHE especially in chemical industries such as brewery and food processing due to their flexibility, compactness, ease of cleaning and assembly/disassembly (Gulenoglu *et al*., 2014).

Choice of gasket materials is critical to the reliable operation of GPHEs. Gaskets are generally made from a variety of elastic and formable materials, such as rubber and its different polymerized forms *(*Wang *et al*., 2007). The gasket materials restrict the use of GPHEs in highly corrosive applications and also limit the maximum operating temperature to avoid the use of expensive gasket materials (Li *et al*., 2011).

Stainless steel is a most commonly used metal for the plates because of its ability to withstand high temperature, its strength, and its corrosion resistance (Wang *et al*., 2007; Durmus *et al*., 2009). The use of high quality metal and the manufacturing techniques lead plate heat exchangers to be less prone to corrosion failure than shell and tube units (Thonon & Breuil, 2000).

The gasket design minimizes the risk of internal leakage. Any failure in the gasket results in leakage to the atmosphere, which is easily detectable on the exterior of the unit. The additional main advantages and benefits offered by the GPHE are (Kakaç *et al*., 2012):

- Flexibility of design through a variety of plate sizes and pass arrangements
- Easily accessible heat transfer area, permitting changes in configuration to suit changes in processes requirements through changes in the number of plates.
- Efficient heat transfer; high heat transfer coefficients for both fluids because of turbulence and a small hydraulic diameter
- Very compact (large heat transfer area/volume ratio), and low in weight; in spite of their compactness, 1,500 m^2 of surface area is available in a single unit
- Only the plate edges are exposed to the atmosphere; the heat losses are negligible and no insulation is required
- Intermixing of the two fluids cannot occur under gasket failure
- Plate units exhibit low fouling characteristics due to high turbulence and low residence time
- More than two fluids may be processed in a single unit.

The transition to turbulence flow occurs at low Reynolds numbers of 10–400. The high turbulence in a GPHE leads to very high transfer coefficients, low fouling rates, and reduced size.

The performance evaluation and rating of gasketed-plate heat exchangers is highly specialized in nature considering the variety of designs available for the plates and arrangements that may possibly suit various duties. Unlike tubular heat exchangers for which design data and methods are easily available, a gasketed-plate heat exchanger design continues to be proprietary in nature. Manufacturers have developed their own computerized design procedures applicable to the exchangers that they market (Kakaç *et al*., 2012).

However, several authors have studied and evaluated the performance of gasketed-plate heat exchangers. In this sense, (Pinto & Gut, 2002) presented an optimization method for determining the best configuration(s) of GPHE, with the objective of selecting the configuration(s) with the minimum heat transfer area that still satisfies constraints on the number of channels, the pressure drop of both fluids, the channel flow velocities and the exchanger thermal effectiveness. Also, (Naik & Matawala, 2013) investigate the characteristics of a GPHE with different Chevron angles and a wide range of Reynolds number, thus carrying out experiments to measure the temperature and mass flow rates at all port with varying flow condition. Similarly, (Gulenoglu *et al*., 2014) utilized an experimental set-up for testing Chevron type gasketed plate heat exchangers to investigate the thermal and hydraulic characteristics of three different plate geometries. The experiments were performed using various numbers of plates, several flow rate and inlet and outlet temperature values so that the Reynolds numbers (300-5000) and Prandtl numbers vary for all the plates that have 30º of Chevron angle. Likewise, (Hajabdollahi *et al*., 2016) presented a comparative study for optimization of gasket-plate and shell and tube heat exchangers, thus selecting the total cost of the system (the capital and operating costs) as objective function and applying Genetic Algorithm to find the minimum of it for each case. Moreover, (Neagu *et al*., 2016) presented comparatively different methods of pressure drop calculation in a GPHE, using correlations recommended in literature on industrial data collected from a vegetable oil refinery. The goal of this study was to compare the results obtained with these correlations, in order to choose one or two for practical purpose of pumping power calculations. In other study, (Turk *et al*., 2016) performed experiments to test the thermal and hydraulic performance of gasketed plate heat exchangers. Other authors (Aradag *et al*., 2017) demonstrated the importance of using corrugation patterns instead of flat plates in the computations of GPHE, and used Artificial Neural Networks estimations for the hydraulic and thermal performance as an alternative to classical correlations. Finally, in (Khan & Jamil, 2018) three plate structures with corrugation angle of 45º, 33.8º and 0º (flat plate) were numerically investigated with water as working fluid and using FLUENT software. Effectiveness, heat transfer rate and thermal hydraulics performance (in term of pressure drop and heat transfer coefficient) were also calculated in this study. Recently, other authors (Dvořák & Vít, 2017; Jamshak *et al*., 2018; Thakkar & Kumar, 2019; Rincón *et al*., 2019; Neagu & Koncsag, 2022) have studied and assessed the performance and operation of GPHEs.

In the present work, the thermo-hydraulic rating of a GPHE proposed for heating a methanol stream was carried out in order to know several important parameters such as the heat exchanged, the safety factor, the cleanliness factor, the percent over surface, the pressure drop and the pumping power required of both streams. To accomplish this objective, the calculation methodology reported by (Kakaç *et al*., 2012) was employed.

2. MATERIALS AND METHODS

2.1. Problem definition

It's necessary to heat 20 kg/s of a methanol stream from 25 ºC to 60 ºC using hot water at 95 ºC. The outlet temperature of the hot water must not be lower than 70 ºC, while the maximum permissible pressure drop for the methanol and water is 80,000 and 50,000 Pa respectively. A GPHE equipped with Chevron plates with the following constructional data is proposed:

- Plate thickness: 0.0006 m.

- Chevron angle: 60 degrees.
- Total number of plates: 104.
- Enlargement factor: 1.25.
- Number of passes: One pass/one pass.
- Total effective area: 108 m^2.
- All port diameters: 0.20 m.
- Compressed plate pack length: 0.38 m.
- Vertical port distance: 1.55 m.
- Horizontal port distance: 0.43 m.
- Effective channel width: 0.63 m.

The plate material is Inconel 600; the flow arrangement will be countercurrent of one pass/one pass type (Figure 2), while the calculated percent over surface should not exceed 25%. Determine if the proposed GPHE is feasible to use for this heat exchange service.

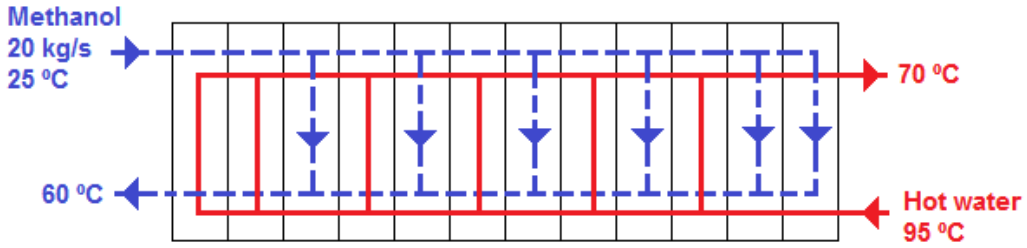

Figure 2. Schematic of the operating conditions for the proposed GPHE

Source: Own elaboration.

2.2. Calculation methodology

To solve the rating problem the calculation methodology published in (Kakaç *et al.*, 2012) was used, where several important parameters such as the safety factor, the percent over surface design, the pressure drop and the pumping power for each stream were calculated. Each of the steps used to carry out the rating of the proposed GPHE are shown below.

Percent over surface:

Step 1. Definition of the initial parameters for both streams:

Table 1 shows the main initial parameters that need to be defined for both streams.

Table 1. Definition of the initial parameters for both streams.

Parameter	Hot fluid	Cold fluid	Units
Mass flowrate	m_h	m_c	kg/s
Inlet temperature	T_1	t_1	°C
Outlet temperature	T_2	t_2	°C
Maximum permissible pressure drop	$\Delta P_{m(h)}$	$\Delta P_{m(c)}$	Pa
Fouling factor	R_h	R_c	m^2.K/W

Source: Own elaboration.

Step 2. Definition of the initial geometrical parameters for the proposed GPHE:

Table 2 presents the main initial geometrical parameters that must be defined for the proposed GPHE, while Figure 3 shows the main dimensions and geometric parameters of the Chevron plate used in this study.

Table 2. Definition of the main initial parameters for the proposed GPHE.

Parameter	Symbol	Units
Plate thickness	t_p	m
Chevron angle	β	º
Total number of plates	N_t	-
Enlargement factor	ϕ	-
Number of passes	N_p	-
Total effective area	A_e	m^2
All port diameters	D_p	m
Compressed plate pack length	L_c	m
Vertical port distance	L_v	m
Horizontal port distance	L_h	m
Effective channel width	L_w	m
Thermal conductivity of the plate material (Inconel 600)	k_p	W/m.K

Source: Own elaboration.

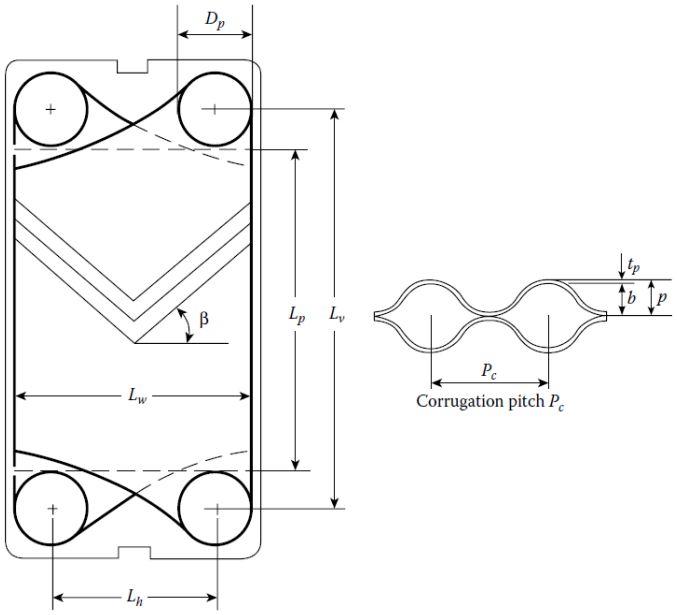

Figure 3. Main dimensions and geometrical parameters of the Chevron plate.
Source: Adapted from (Kakaç et al., 2012).

Step 3. Mean temperature for both streams:

Hot fluid:

$$\overline{T} = \frac{T_1 + T_2}{2} \tag{1}$$

Cold fluid:

$$\bar{t} = \frac{t_1 + t_2}{2} \tag{2}$$

Step 4. Physical properties for both streams at the mean temperature determined in Step 3:

Table 3 displays the physical properties that must be determined for both streams at the mean temperature calculated in Step 3.

Table 3. Physical properties for both streams at the mean temperature calculated in step 3.

Physical property	Hot fluid	Cold fluid	Units
Specific heat	Cp_h	Cp_c	J/kg.K
Density	ρ_h	ρ_c	kg/m^3
Viscosity	μ_h	μ_c	Pa.s
Thermal conductivity	k_h	k_c	W/m.K

Source: Own elaboration.

Step 5. Required heat load (Q):

Hot fluid:

$$Q = m_h \cdot Cp_h \cdot (T_1 - T_2) \tag{3}$$

Cold fluid:

$$Q = m_c \cdot Cp_c \cdot (t_2 - t_1) \tag{4}$$

Step 6. Mean temperature difference (ΔT_m):

For countercurrent flow:

$$\Delta T_m = \frac{(T_1 - t_2) - (T_2 - t_1)}{\ln \dfrac{(T_1 - t_2)}{(T_2 - t_1)}} \tag{5}$$

Step 7. Effective number of plates (N_e):

$$N_e = N_t - 2 \tag{6}$$

Step 8. Effective flow length between the vertical ports (L_{eff}):

$$L_{eff} \approx L_v \tag{7}$$

Step 9. Plate pitch (p):

$$p = \frac{L_c}{N_t} \tag{8}$$

Step 10. Mean channel flow gap (b):

$$b = p - t_p \tag{9}$$

Step 11. One channel flow area (A_{ch}):

$$A_{ch} = b \cdot L_w \tag{10}$$

Step 12. Single-plate heat transfer area (A_1):

$$A_1 = \frac{A_e}{N_e} \tag{11}$$

Step 13. Projected plate area (A_{1p}):

$$A_{1p} = \left(L_v - D_p\right) \cdot L_w \tag{12}$$

Step 14. Calculated enlargement factor (ϕ):

$$\phi = \frac{A_1}{A_{1p}} \tag{13}$$

Step 15. Channel hydraulic/equivalent diameter (D_h):

$$D_h = \frac{2 \cdot b}{\phi} \tag{14}$$

Step 16. Number of channels per pass (N_{cp}):

$$N_{cp} = \frac{N_t - 1}{2 \cdot N_p} \tag{15}$$

Step 17. Mass flowrate per channel:

Hot fluid ($m_{c(h)}$):

$$m_{c(h)} = \frac{m_h}{N_{cp}} \tag{16}$$

Cold fluid ($m_{c(c)}$):

$$m_{c(c)} = \frac{m_c}{N_{cp}} \tag{17}$$

Step 18. Mass velocity:

Hot fluid (G_h):

$$G_h = \frac{m_{c(h)}}{A_{ch}} \tag{18}$$

Cold fluid (G_c):

$$G_c = \frac{m_{c(c)}}{A_{ch}} \tag{19}$$

Step 19. Reynolds number:

Hot fluid (Re_h):

$$\mathrm{Re}_h = \frac{G_h \cdot D_h}{\mu_h} \tag{20}$$

Cold fluid (Re_c):

$$\mathrm{Re}_c = \frac{G_c \cdot D_h}{\mu_c} \tag{21}$$

Step 20. Prandtl number:

Hot fluid (Pr_h):

$$\mathrm{Pr}_h = \frac{Cp_h \cdot \mu_h}{k_h} \tag{22}$$

Cold fluid (Pr_c):

$$\mathrm{Pr}_c = \frac{Cp_c \cdot \mu_c}{k_c} \tag{23}$$

Step 21. Film heat transfer coefficient:

Hot fluid (h_h):

$$h_h = \frac{k_h}{D_h} \cdot C_h \cdot \mathrm{Re}_h^n \cdot \mathrm{Pr}_h^{0.33} \cdot \left(\frac{\mu_h}{\mu_{hw}} \right)^{0.17} \tag{24}$$

Cold fluid (h_c):

$$h_c = \frac{k_c}{D_h} \cdot C_h \cdot \mathrm{Re}_c^n \cdot \mathrm{Pr}_c^{0.33} \cdot \left(\frac{\mu_c}{\mu_{cw}} \right)^{0.17} \tag{25}$$

Where C_h and n are constants that depend on the angle of the Chevron plate and the Reynolds number, and are reported in Table 11.6, page 472 (Kakaç et al., 2012).

Step 22. Clean overall heat transfer coefficient (U_C):

$$U_C = \frac{1}{\frac{1}{h_h} + \frac{1}{h_c} + \frac{t_p}{k_p}} \tag{26}$$

Step 23. Fouled overall heat transfer coefficient (U_F):

$$U_F = \frac{1}{\frac{1}{U_C} + R_h + R_c} \tag{27}$$

Step 24. Cleanliness factor (CF):

$$CF = \frac{U_F}{U_C} \tag{28}$$

Step 25. Actual heat duty for clean surface (Q_C):

$$Q_C = U_C \cdot A_e \cdot \Delta T_m \tag{29}$$

Step 26. Actual heat duty for fouled surface (Q_F):

$$Q_F = U_F \cdot A_e \cdot \Delta T_m \tag{30}$$

Step 27. Safety factor (C_s):

$$C_s = \frac{Q_F}{Q} \tag{31}$$

Step 28. Percent over surface (OS):

$$OS = 100 \cdot U_C \cdot \left(R_h + R_c\right) \tag{32}$$

Pressure drop:

The pressure drop of the fluids that circulate inside a GPHE is constituted by two types of pressure drops, that is: 1) the frictional pressure drop, and 2) the pressure drop in the port ducts (Kakaç et al., 2012). Next, the calculation methodology employed to determine the overall pressure drop for each fluid stream is presented.

Step 29. Friction coefficient:

Hot fluid (f_h):

$$f_h = \frac{K_p}{\mathrm{Re}_h^m} \tag{33}$$

Cold fluid (f_c):

$$f_c = \frac{K_p}{\mathrm{Re}_c^m} \tag{34}$$

Where K_p and m are given in Table 11.6, page 472 (Kakaç et al., 2012) as function of Reynolds number for various values of Chevron angles.

Step 30. Frictional pressure drop:

Hot fluid [$\Delta P_{f(h)}$]:

$$\Delta P_{f(h)} = 4 \cdot f_h \cdot \frac{L_{eff} \cdot N_p}{D_h} \cdot \frac{G_h^2}{2 \cdot \rho_h} \cdot \left(\frac{\mu_h}{\mu_{hw}} \right)^{-0.17} \tag{35}$$

Cold fluid [$\Delta P_{f(c)}$]:

$$\Delta P_{f(c)} = 4 \cdot f_c \cdot \frac{L_{eff} \cdot N_p}{D_h} \cdot \frac{G_c^2}{2 \cdot \rho_c} \cdot \left(\frac{\mu_c}{\mu_{cw}} \right)^{-0.17} \tag{36}$$

Step 31. Port mass velocity:

Hot fluid ($G_{p(h)}$):

$$G_{p(h)} = \frac{m_h}{\frac{\pi \cdot D_p^2}{4}} \tag{37}$$

Cold fluid ($G_{p(c)}$):

$$G_{p(c)} = \frac{m_c}{\frac{\pi \cdot D_p^2}{4}} \tag{38}$$

Step 32. Pressure drop in the port ducts:

Hot fluid ($\Delta P_{p(h)}$):

$$\Delta P_{p(h)} = 1.4 \cdot N_p \cdot \frac{G_{p(h)}^2}{2 \cdot \rho_h} \tag{39}$$

Cold fluid ($\Delta P_{p(c)}$):

$$\Delta P_{p(c)} = 1.4 \cdot N_p \cdot \frac{G_{p(c)}^2}{2 \cdot \rho_c} \tag{40}$$

Step 33. Total pressure drop:

Hot fluid (ΔP_h):

$$\Delta P_h = \Delta P_{f(h)} + \Delta P_{p(h)} \tag{41}$$

Cold fluid (ΔP_c):

$$\Delta P_c = \Delta P_{f(c)} + \Delta P_{p(c)} \tag{42}$$

Step 34. Pumping power required:

Hot fluid (P_h):

$$P_h = \frac{\Delta P_h \cdot m_h}{\eta_p \cdot \rho_h} \tag{43}$$

Cold fluid (P_c):

$$P_c = \frac{\Delta P_c \cdot m_c}{\eta_p \cdot \rho_c} \tag{44}$$

Where η_p is the isentropic efficiency of the adiabatic pump, and a value of 0.8 was considered for this parameter in this study (Kakaç et al., 2012).

3. RESULTS AND DISCUSSION

Percent over surface:

Step 1. Definition of the initial parameters for both streams:

Table 4 indicates the values of the initial parameters defined for both streams.

Table 4. Values of the initial parameters defined for both streams.

Parameter	Water	Methanol	Units
Mass flowrate	-	90	kg/s
Inlet temperature	95	25	ºC
Outlet temperature	70	60	ºC
Maximum permissible pressure drop	50,000	80,000	Pa
Fouling factor†	0.0000086	0.0000034	m^2.K/W

†Taken from (Kakaç et al., 2012).
Source: Own elaboration.

Step 2. Definition of the initial parameters for the proposed GPHE:

Table 5 specifies the values of the initial parameters defined for the proposed GPHE.

Table 5. Values of the initial parameters defined for the proposed GPHE.

Parameter	Symbol	Value	Units
Plate thickness	t_p	0.0006	m
Chevron angle	β	60	º
Total number of plates	N_t	105	-
Enlargement factor	ϕ	1.25	-

Number of passes	N_p	1	-
Total effective area	A_e	108	m^2
All port diameters	D_p	0.2	m
Compressed plate pack length	L_c	0.38	m
Vertical port distance	L_v	1.55	m
Horizontal port distance	L_h	0.43	m
Effective channel width	L_w	0.63	m
Thermal conductivity of the plate material (Inconel 600)[§]	k_p	16	W/m.K

[§] Taken from (Raju & Jagdish, 1983).
Source: Own elaboration.

Step 3. Mean temperature for both streams:

Hot fluid:

$$\bar{T} = \frac{T_1 + T_2}{2} = \frac{95 + 70}{2} = 82.5\,^{o}C$$

Cold fluid:

$$\bar{t} = \frac{t_1 + t_2}{2} = \frac{25 + 60}{2} = 42.5\,^{o}C$$

Step 4. Physical properties for both streams at the mean temperature determined in step 3:

According to (Green & Southard, 2019) both the hot water and methanol present the values of the physical properties described in Table 6 at the mean temperature calculated in step 3.

Table 6. Values of the physical properties determined for both streams at the mean temperature calculated in step 3.

Physical property	Water	Methanol	Units
Specific heat	4,198.36	2,641.32	J/kg.K
Density	971.54	772.47	kg/m^3
Viscosity	0.00034	0.00043	Pa.s
Thermal conductivity	0.6662	0.1950	W/m.K

Source: Own elaboration.

Step 5. Required heat load (Q):

Using equation (4) since it's the one that presents the complete data:

$$Q = m_c \cdot Cp_c \cdot (t_2 - t_1) = 90 \cdot 2{,}641.32 \cdot (60 - 25)$$
$$Q = 8{,}320{,}158\,W$$

Then, the required mass flowrate of the hot water required by the heat transfer service is:

$$m_h = \frac{Q}{Cp_h \cdot (T_1 - T_2)} = \frac{8{,}320{,}158}{4{,}198.36 \cdot (95 - 70)} = 79.27\ kg/s$$

Table 7 shows the numeric results of the parameters calculated in steps 6-16.

Table 7. Numeric results of the parameters calculated in steps 6-16.

Step	Parameter	Symbol	Value	Units
6	Mean temperature difference (for countercurrent flow)	ΔT_m	39.84	ºC
7	Effective number of plates	N_e	103	-
8	Effective flow length between the vertical ports	L_{eff}	1.55	m
9	Plate pitch	p	0.00362	m
10	Mean channel flow gap	b	0.00302	m
11	One channel flow area	A_{ch}	0.0019	m^2
12	Single-plate heat transfer area	A_1	1.049	m^2
13	Projected plate area	A_{1p}	0.8505	m^2
14	Calculated enlargement factor	ϕ	1.233	-
15	Channel hydraulic/equivalent diameter	D_h	0.0049	m
16	Number of channels per pass	N_{cp}	52	-

Source: Own elaboration.

Table 8 displays the results of the parameters determined in steps 17-20.

Table 8. Results of the parameters determined in steps 17-20.

Step	Parameter	Water	Methanol	Units
17	Mass flowrate per channel	1.524	1.731	kg/s
18	Mass velocity	802.10	911.05	$kg/m^2.s$
19	Reynolds number	11,559.67	10,381.73	-
20	Prandtl number	2.14	5.82	-

Source: Own elaboration.

Step 21. Film heat transfer coefficient:

For hot water:

$$h_h = \frac{k_h}{D_h} \cdot C_h \cdot \mathrm{Re}_h^n \cdot \mathrm{Pr}_h^{0.33} \cdot \left(\frac{\mu_h}{\mu_{hw}} \right)^{0.17}$$

Where C_h = 0.108 and n = 0.703 as reported by (Kakaç et al., 2012) since Re_h > 400 and β = 60, while it's assumed that the ratio $(\mu_h/\mu_{hw})^{0.17}$ = 1 (Kakaç et al., 2012). Then:

$$h_h = \frac{0.6662}{0.0049} \cdot 0.108 \cdot 11{,}559.67^{0.703} \cdot 2.14^{0.33} \cdot 1$$
$$h_h = 13{,}551.56\, W/m^2.K$$

For methanol:

$$h_c = \frac{k_c}{D_h} \cdot C_h \cdot \mathrm{Re}_c^n \cdot \mathrm{Pr}_c^{0.33} \cdot \left(\frac{\mu_c}{\mu_{cw}} \right)^{0.17}$$

Where C_h = 0.108 and n = 0.703 as reported by (Kakaç et al., 2012) since Re_c > 400 and β = 60, while it's assumed that the ratio $(\mu_c/\mu_{cw})^{0.17}$ = 1 (Kakaç et al., 2012). Then:

$$h_c = \frac{0.1950}{0.0049} \cdot 0.108 \cdot 10{,}381.73^{0.703} \cdot 5.82^{0.33} \cdot 1$$
$$h_c = 5{,}116.82\, W/m^2.K$$

Table 9 depicts the results of the parameters determined in steps 22-28.

Table 9. Results of the parameters determined in steps 22-28.

Step	Parameter	Symbol	Value	Units
22	Clean overall heat transfer coefficient	U_C	3,260.24	W/m^2.K
23	Fouled overall heat transfer coefficient	U_F	3,137.49	W/m^2.K
24	Cleanliness factor	CF	0.962	-
25	Actual heat duty for clean surface	Q_C	14,027,899.85	W
26	Actual heat duty for fouled surface	Q_F	13,499,740.97	W
27	Safety factor	C_s	1.62	-
28	Percent over surface	OS	3.91	%

Source: Own elaboration.

Pressure drop:

Step 29. Friction coefficient:

Hot water:

$$f_h = \frac{K_p}{\mathrm{Re}_h^m}$$

Where K_p = 0.760 and m = 0.215 as reported by (Kakaç et al., 2012) since Re_h > 400 and β = 60. Then:

$$f_h = \frac{0.760}{11{,}559.67^{0.215}} = 0.1017$$

Methanol:

$$f_c = \frac{K_p}{\mathrm{Re}_c^m}$$

Where K_p = 0.760 and m = 0.215 as reported by (Kakaç et al., 2012) since Re_c > 400 and β = 60. Then:

$$f_c = \frac{0.760}{10{,}381.73^{0.215}} = 0.1040$$

Table 10 indicates the results of the parameters determined in steps 30-34. In the case of the equations (35) and (36), corresponding to the step 30, the ratios $(\mu_h/\mu_{hw})^{-0.17}$ and $(\mu_c/\mu_{cw})^{-0.17}$ are considered equal to 1, according to (Kakaç et al., 2012).

Table 10. Results of the parameters calculated in steps 30-34.

Step	Parameter	Water	Methanol	Units
30	Frictional pressure drop	42,607.12	70,697.01	Pa
31	Port mass velocity	2,524.52	2,866.24	kg/m^2.s
32	Pressure drop in the port ducts	4,591.93	7,444.60	Pa
33	Total pressure drop	47,199.05	78,141.61	Pa
34	Pumping power required	4,813.84	11,380.29	W

Source: Own elaboration.

According to the results obtained, the required heat load had a value of 8,320,158 W, and 79.27 kg/s of hot water are needed to satisfy the thermal demand of the gasketed-plate heat exchanger. Both fluids will circulate through the heat exchanger under turbulent flow, due to the values obtained of the Reynolds number, which were 11,559.67 and 10,381.73 for water and methanol, respectively. It is worth noting that the Reynolds number of water is 1.11 times higher than the Reynolds number of methanol, which is mainly due to the lower viscosity of water (0.00034 Pa.s) compared to that of the methanol (0 .00043 Pa.s).

For its part, the film heat transfer coefficient of hot water (13,551.56 W/m^2.K) was 2.65 times higher than the film heat transfer coefficient of methanol (5,116.82 W/m^2.K), essentially due to the higher value of the parameters Reynolds number and thermal conductivity that presents the water with respect to methanol. A value of the clean overall heat transfer coefficient of 3,260.24 W/m^2.K was also obtained, which is 1.04 times higher than the value obtained for the fouled overall heat transfer coefficient (3,137.49 W/m^2.K). The cleanliness factor had a value of 0.962, while the value obtained for the safety factor was 1.62, which can be considered acceptable (Kakaç et al., 2012). Finally, the value obtained for the percent over surface was 3.91%, which is below the maximum permissible limit established by the process (25%). Taking into account the above, the proposed gasketed-plate heat exchanger can be considered adequate from a thermal point of view.

Regarding pressure drops, the frictional pressure drop of methanol (70,697.01 Pa) is 1.66 times higher than the frictional pressure drop of hot water (42,607.12 Pa), mainly due to the lower density that presents

methanol (772.47 kg/m^3) with respect to water (971.54 kg/m^3) and the highest value of the mass velocity of methanol (911.05 kg/m^2.s) in relation to the mass velocity of water (802.10 kg/m^2.s). Regarding the pressure drop in the port ducts, the calculated value of this parameter for methanol was 7,444.60 Pa, which is 1.62 times greater than the pressure drop in the port ducts for the hot water (4,591.93 Pa). This is fundamentally due to the higher port mass velocity that methanol presents (2,866.24 kg/m^2.s) with respect to that of water (2,524.52 kg/m^2.s), and also to the lower density that presents methanol with respect to that of water. Therefore, the total pressure drop of methanol (78,141.61 Pa) is 1.65 times higher than the total pressure drop of hot water (47,199.05), thus concluding that the proposed heat exchanger is adequate from the hydraulic point of view, since the total pressure drops of both streams are below the maximum allowable pressure drop established by the process, which is 50,000 Pa and 80,000 Pa for water and methanol, respectively.

Finally, the pumping power required for methanol was 11.38 kW, which is 2.36 times higher than the pumping power required for hot water (4.81 kW). This is basically due to the greater total pressure drop that the methanol presents with respect to the total pressure drop of hot water, which was discussed previously.

4. CONCLUSIONS

The required heat load had a value of 8,320,158 W, and 79.27 kg/s of hot water will be needed to meet the thermal duty of the system.

The film heat transfer coefficient of hot water (13,551.56 W/m^2.K) was 2.65 times higher than the value of this parameter for methanol (5,116.82 W/m^2.K).

A value for the cleanliness factor and the safety factor of 0.962 and 1.62 were obtained respectively, which can be considered acceptable.

The value obtained for the percent over surface was 3.91%, which is below the maximum permissible limit established by the process.

The total pressure drop of methanol (78,141.61 Pa) was 1.65 times higher than the total pressure drop of hot water (47,199.05 Pa), while both values are below the maximum allowable limit established by the process for the two streams.

A pumping power of 11.38 kW and 4.81 kW will be required for the methanol and hot water, respectively.

It is concluded that the proposed gasketed-plate heat exchanger is feasible to use from the thermo-hydraulic point of view, since the calculated values of the percent over surface and both pressure drops are below the maximum limits established by the heat exchange service.

REFERENCES

Aradag, S., Genc, Y., and Turk, C. (2017). Comparative gasketed plate heat exchanger performance prediction with computations, experiments, correlations and artificial neural network estimations. Engineering Applications of Computational Fluid Mechanics, 11 (1), 467-482. doi:10.1080/19942060.2017.1314870.

Dovic, D., Palm, B., and Švaic, S. (2009). Generalized correlations for predicting heat transfer and pressure drop in plate heat exchanger channels of arbitrary geometry. International Journal of Heat and Mass Transfer, 52, 4553–4563. doi:10.1016/j.ijheatmasstransfer.2009.03.074.

Durmus, A., Benli, H., Kurtbas, I., and Gül, H. (2009). Investigation of heat transfer and pressure drop in plate heat exchangers having different surface profiles. International Journal of Heat and Mass Transfer, 52, 1451–1457. doi:10.1016/j.ijheatmasstransfer.2008.07.052.

Dvořák, V., and Vít, T. (2017). Evaluation of CAE methods used for plate heat exchanger design. Energy Procedia, 111, 141 – 150. doi:10.1016/j.egypro.2017.03.016.

Elshafei, E. A. M., Awad, M. M., El-Negiry, E., and Ali, A. G. (2010). Heat transfer and pressure drop in corrugated channels. Energy, 35, 101–110. doi:10.1016/j.energy.2009.08.031.

Green, D. W., and Southard, M. Z. (2019). Perry's Chemical Engineers' Handbook (9th ed.). New York, U.S.A.: McGraw-Hill.

Gulenoglu, C., Akturk, F., Aradag, S., Uzol, N. S., and Kakac, S. (2014). Experimental comparison of performances of three different plates for gasketed plate heat exchangers. International Journal of Thermal Sciences, 75, 249-256. doi:10.1016/j.ijthermalsci.2013.06.012.

Hajabdollahi, H., Naderi, M., and Adimi, S. (2016). A comparative study on the shell and tube and gasket-plate heat exchangers: The economic viewpoint. Applied Thermal Engineering, 92, 271-282. doi:10.1016/j.applthermaleng.2015.08.110.

Heggs, P. J., Sandham, P., Hallam, R. A., and Walton, C. (1997). Local transfer coefficients in corrugated plate heat exchangers channels. Chemical Engineering Research and Design, 75 (7), 641-645. doi:10.1205/026387697524254.

Jamshak, S. H., Anand, M. D., Akshay, S. B., Arun, S., Prajeev, J., and Prabhakaran, P. (2018). Design and Analysis of a Plate Heat Exchanger in the View of Performance Improvement and Cost Reduction. International Journal of Engineering & Technology, 7 (3.27), 440-446.

Kakaç, S., Liu, H., and Pramuanjaroenkij, A. (2012). Heat Exchangers - Selection, Rating and Thermal Design (3rd ed.). Boca Raton, U.S.A: CRC Press.

Khan, M. S., and Jamil, Z. (2018). Analysis of corrugation angle on thermal performance of plate heat exchanger. Academia Journal of Scientific Research, 6 (10), 1-11. doi:10.15413/ajsr.2018.0160.

Li, Q., Flamant, G., Yuan, X., Neveu, P., and Luo, L. (2011). Compact heat exchangers: A review and future applications for a new generation of high temperature solar receivers. Renewable and Sustainable Energy Reviews, 15, 4855– 4875. doi:10.1016/j.rser.2011.07.066.

Mota, F. A. S., Carvalho, E. P., and Ravagnani, M. A. S. S. (2015). Chapter 7. Modeling and Design of Plate Heat Exchanger. In S. N. Kazi (Ed.), Heat Transfer Studies and Applications: AvE4EvA.

Naik, V. R., and Matawala, V. K. (2013). Experimental Investigation of Single Phase Chevron Type Gasket Plate Heat Exchanger. International Journal of Engineering and Advanced Technology, 2 (4), 362-369.

Neagu, A. A., and Koncsag, C. I. (2022). Model Validation for the Heat Transfer in Gasket Plate Heat Exchangers Working with Vegetable Oils. Processes, 10 (1), 102. doi:10.3390/pr10010102.

Neagu, A. A., Koncsag, C. I., Barbulescu, A., and Botez, E. (2016). Estimation of pressure drop in gasket plate heat exchangers. Ovidius University Annals of Chemistry, 27 (1), 62-72. doi:10.1515/auoc-2016-0011.

Pinto, J. M., and Gut, J. A. W. (2002). A Screening method for the optimal selection of plate heat exchanger configuration. Brazilian Journal of Chemical Engineering, 19 (4), 433-439.

Raju, K. S. N., and Jagdish, C. B. (1983). Low Reynolds Number Flow Heat Exchangers. Washington DC, U.S.A.: Hemisphere.

Rincón, J. S., Perdomo-Hurtado, L., and Aragón, J. L. (2019). Study of Gasketed-Plate Heat Exchanger performance based on energy efficiency indexes. Applied Thermal Engineering, 159, 113902. doi:10.1016/j.applthermaleng.2019.113902.

Shah, R. K., and Sekulic, D. P. (2003). Fundamentals of heat exchanger design. New Jersey, U.S.A: John Wiley & Sons.

Thakkar, N. P., and Kumar, M. (2019). Performance Analysis and Optimization of Plate Type Heat Exchanger in Dairy Industries. PDPU Journal of Energy and Management, 3 (2), 11-20.

Thonon, B., and Breuil, E. (2000). Compact Heat Exchanger Technologies for the HTRs Recuperator Application. Paper presented at the IAEA-TECDOC, Palo Alto, California.

Turk, C., Aradag, S., and Kakac, S. (2016). Experimental analysis of a mixed-plate gasketed plate heat exchanger and artificial neural net estimations of the performance as an alternative to classical correlations. International Journal of Thermal Sciences, 109, 263-269. doi:10.1016/j.ijthermalsci.2016.06.016.

Wang, L., Sundén, B., and Manglik, R. M. (2007). Plate Heat Exchangers - Design, Applications and Performance. Southampton, U.K.: WIT Press.

Würfel, R., and Ostrowski, N. (2004). Experimental investigations of heat transfer and pressure drop during the condensation process within plate heat exchangers of the herringbone-type. International Journal of Thermal Sciences, 43, 59-68. doi:10.1016/S1290-0729(03)00099-1.

SEMBLANCE OF THE AUTHORS

Amaury Pérez Sánchez: Obtained a degree in Chemical Engineering from the University of Camagüey, Cuba in 2009, where he is currently an instructor professor and assistant researcher. At the moment he is studying a Master in Biotechnology at the Center for Genetic Engineering and Biotechnology in Camagüey. He works in research lines related fundamentally with the design of heat and mass transfer equipment, simulation and optimization of processes and operations in the chemical industry using simulators such as SuperPro Designer® and ChemCAD®, and the techno-economic evaluation of processes and biotechnological plants.

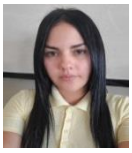

Helen María Alfonso Fernández: Obtained a degree in Chemical Engineering from the University of Camagüey, Cuba in 2018, where she is currently an instructor professor. At present, she is studying a Master in Chemical Processes Analysis at the University of Camagüey. Her research areas involve the design/assessment of heat and mass transfer equipment and biologic reactors, as well as the techno-economic evaluation of chemical and biotechnological plants using SuperPro Designer® simulator.

Greisy Ivety Valero Almanza: Obtained a degree in Chemical Engineering form the University of Camagüey, Cuba in 2019. She works professionally as a Science, Technology and Environmental Specialist in the Environmental Management Department of the Environmental Engineering Center of Camagüey. Her research area includes studies of environmental risks in chemical companies and plants, environmental management of residuals and chemical waste, physical-chemical analysis of water and wastewater, as well as the design and evaluation of heat and mass transfer equipment.

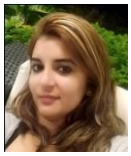

Elizabeth Ranero González: Obtained a degree of Chemical Engineering from the University of Camagüey, Cuba in 2016. She works professionally as Instructor Professor at the University of Camagüey, Cuba. Her research area includes the design and rating of heat and mass transfer equipment and processes, thermodynamic evaluation of chemical processes, and the simulation of biotechnological processes.

Eddy Javier Pérez Sánchez: Obtained a degree in Chemical Engineering from the University of Camagüey, Cuba in 2016. He works professionally at Empresa de Servicios Automotores S.A., in the Department of Commercial Management. His research topics involve the design and rating of heat and mass transfer equipment, as well as the simulation of petrochemical and biotechnological processes.